Proteasome inhibitor MG132 modulates signal transduction pathways in ELT3 uterine leiomyoma cells

HOSOUK JOUNG[1], SO-RA YANG[2,3], SU BIN LEE[2] and HYUNJU LIU[2,3]

[1]Research Institute of Medical Sciences, Chonnam National University Medical School, Hwasun, Jeollanam-do 58128, Republic of Korea; [2]Department of Obstetrics and Gynecology, Chosun University Hospital, Gwangju 61453, Republic of Korea; [3]Department of Obstetrics and Gynecology, Chosun University College of Medicine, Gwangju 61452, Republic of Korea

Received October 17, 2024; Accepted January 29, 2025

DOI: 10.3892/etm.2025.12821

Abstract. Uterine leiomyomas, or fibroids, are common benign tumors that affect a significant percentage of women, with treatment options ranging from medication to surgery. Carbobenzoxyl-L-leucyl-L-leucyl-L-leucine (MG132), a proteasome inhibitor, has exhibited potential in treating various cancers by disrupting key cellular processes such as apoptosis and cell cycle regulation. The present study aimed to evaluate the effects of MG132 on the viability, proliferation, apoptosis, and the production of reactive oxygen species (ROS) in Eker leiomyoma tumor-3 (ELT3) uterine leiomyoma cells and to elucidate the underlying molecular mechanisms involved. Cell viability was evaluated using an MTT assay, while cytotoxicity was assessed using a lactate dehydrogenase (LDH) release assay. Colony formation assays assessed the long-term effects of MG132. Apoptosis and cell cycle distribution were analyzed using flow cytometry with Annexin V staining, and ROS production was also measured by flow cytometry. Western blot analysis was performed to examine key proteins related to the cell cycle and apoptosis. The findings of the present study revealed that MG132 significantly reduced the cell viability and impaired colony formation in ELT3 cells, as evidenced by decreased cell viability and increased LDH activity. MG132 treatment significantly increased apoptosis and induced cell cycle arrest at the G_2/M phase. Additionally, MG132 increased the levels of ROS, which contributed to ROS-mediated apoptosis. Western blot analysis revealed that MG132 modulated key proteins involved in cell proliferation and apoptosis, including p21, p27, ERK, and caspase-3. Furthermore, MG132 treatment induced autophagy, as indicated by the increased conversion of LC3 I to LC3 II. Overall, MG132 was revealed to exert potent cytotoxic effects on ELT3 uterine leiomyoma cells by inducing ROS-mediated apoptosis and cell cycle arrest, and triggering autophagy. These findings suggest that MG132 provides a proof of concept for targeting the proteasome in uterine leiomyomas.

Correspondence to: Professor Hyunju Liu, Department of Obstetrics and Gynecology, Chosun University College of Medicine, 309 Pilmun-daero, Dong-gu, Gwangju 61452, Republic of Korea
E-mail: lhj@chosun.ac.kr

Abbreviations: MG132, carbobenzoxyl-L-leucyl-L-leucyl-L-leucine; ELT3, Eker leiomyoma tumor-3; Ut-SMCs, uterine smooth muscle cells; LDH, lactate dehydrogenase; ROS, reactive oxygen species; NAC, N-acetylcysteine; ERK, extracellular signal-regulated kinase; Hsp90, heat shock protein 90; LC3, microtubule-associated protein 1 light chain 3

Key words: uterine, leiomyoma, fibroid, MG132, proliferation, apoptosis, autophagy

Introduction

Uterine leiomyomas, also known as fibroids, are benign tumors that arise from the smooth muscle tissue of the uterus (1,2). They are found in 20-30% of women during their reproductive years and affect 40-50% of women over the age of 35, making them a prevalent condition (3). Although the exact cause of uterine fibroids remains unknown, they are believed to originate from a single abnormal cell within the smooth muscle of the uterine (4). Clinical symptoms manifest in 20-50% of affected individuals and vary depending on the number, size, and location of the fibroids (5). Common symptoms include abnormal uterine bleeding, pelvic pain or pressure, decreased bladder capacity, constipation, and reproductive dysfunction (6,7).

Treatment options for uterine fibroids include medication, surgical interventions, and non-surgical approaches (8,9). Medication aims to regulate hormone levels to inhibit fibroid growth and alleviate symptoms (2). Surgical treatments are considered when the fibroids are large, or the symptoms are severe, and include myomectomy and hysterectomy (10). Non-surgical treatments, such as uterine artery embolization and high-intensity focused ultrasound, are also available (11,12). The choice of treatment depends on factors such as the health condition, age, menopausal status, and symptom severity of the patient. It is crucial for patients to have a detailed consultation with a healthcare provider before deciding on the appropriate treatment approach.

Recent developments in proteasome-targeting drugs have drawn attention as potential therapeutic agents for gynecological diseases, however the literature currently

provides limited data on this topic. Proteasome inhibitors, such as bortezomib, have been explored in combination with chemotherapy for various cancers, including breast cancer and other solid tumors. For instance, bortezomib has been tested with agents such as paclitaxel, capecitabine, and docetaxel for metastatic breast cancer, but the results have been disappointing in terms of efficacy (13-15). Furthermore, bortezomib did not exhibit significant improvements when combined with standard treatments for ovarian cancer (16). A Phase I trial also investigated the combination of bortezomib and chemoradiation for cervical cancer, indicating that while proteasome inhibitors have been tested in gynecological cancers, the results have largely been exploratory and have not demonstrated clear clinical benefits (17). In summary, although there has been some investigation of proteasome-targeting drugs for gynecological malignancies, these trials remain limited and have not provided compelling evidence of significant efficacy thus far.

Carbobenzoxyl-L-leucyl-L-leucyl-L-leucine (MG132) is a potent, reversible, and cell-permeable proteasome inhibitor that interferes with the activity of the 26S proteasome, thereby blocking the degradation of ubiquitin-conjugated proteins (18). This inhibition prevents the breakdown of misfolded, damaged, or regulatory proteins, leading to their accumulation within the cell and disrupting key processes, such as cell cycle progression, apoptosis, and signal transduction pathways (19-21). Notably, MG132 has been reported to affect several types of cancers, including breast, prostate, and liver cancers (22-24). By stabilizing ubiquitinated proteins, MG132 allows researchers to study their roles in cellular functions. Widely used in cancer research, MG132 aids in studying apoptosis evasion mechanisms (20) and uncontrolled proliferation in cancer cells (25). It is also valuable in studying neurodegenerative diseases, where protein aggregation plays a key role (26). Overall, MG132 is essential for investigating protein degradation dynamics and their implications in various diseases, providing potential avenues for therapeutic development.

Despite the potential of MG132, its effects on uterine leiomyoma cells have not been fully investigated. The present study examined the potential of proteasome inhibition using MG132 in Eker leiomyoma tumor-3 (ELT3) uterine leiomyoma cells, focusing on its mechanisms of action, including cell cycle arrest, induction of apoptosis, and the role of reactive oxygen species (ROS) in mediating these effects. The findings of the present study may contribute to the development of more specific and safer proteasome-targeting drugs for clinical application in uterine leiomyomas.

Materials and methods

Cell lines and reagents. The rat leiomyoma cell line, ELT3, was obtained from the American Type Culture Collection. Human uterine smooth muscle cells (Ut-SMCs) were purchased from PromoCell GmbH. Both cell lines were cultured in DMEM (cat. no. LM001-05; Welgene, Inc.) with 10% fetal bovine serum (cat. no. SH30919.03; Hyclone; Cytiva) and 1% streptomycin-penicillin (cat. no. 15140122; Gibco; Thermo Fisher Scientific, Inc.), and maintained in a humidified incubator at 37˚C with 5% CO_2. MG132 was sourced from Selleck Chemicals (cat. no. S2619). N-acetyl-L-cysteine (NAC; cat. no. A7250) was purchased from MilliporeSigma. NAC was used alone or in combination with MG132 to determine the role of ROS production in MG132-induced apoptosis. Dimethyl sulfoxide (cat. no. DMS555.500; BioShop Canada Inc.) served as the control.

MTT and lactate dehydrogenase (LDH) release assay. MTT and LDH release assays assessed cell viability and cytotoxicity, respectively. MTT and LDH release assays were performed according to previously established methods (27). Briefly, ELT3 cells ($5.0x10^3$ cells per well) were seeded in 96-well plates for 24 h and then were treated with varying concentrations of MG132 for either 24 or 48 h. In the MTT assay, the resulting formazan crystals were dissolved by adding 150 μl dimethyl sulfoxide to each well, and the absorbance was measured at 570 nm. The absorbance values were normalized to the control group to determine the relative viability of the treated cells compared with the untreated controls.

Colony formation assay. ELT3 cells were seeded in 6-well plates at 1,000 cells per well and incubated for 24 h at 37˚C and 5% CO_2. Following incubation, the medium was replaced with fresh medium containing varying concentrations of MG132 (0, 0.25, 0.5, 1 and 2 μM), and the cells were incubated at 37˚C for 5 days to allow colony formation. Colony growth was assessed using a crystal violet assay kit (ab232855; Abcam) as per the manufacturer's instructions. Colonies were stained with 2% crystal violet solution at room temperature for 20 min, washed with distilled water, and air-dried. The stained cells were dissolved in a solubilization solution (included in the aforementioned kit), and the absorbance was measured at 570 nm using an INNO microplate reader (LTEK Co., Ltd.) to quantify colony formation and analyze the effect of MG132.

Flow cytometric analysis of apoptosis. The apoptotic profiles of ELT3 cells were measured using a Muse® Annexin V & Dead Cell Kit (cat. no. MCH100105; Cytek Biosciences) following the protocol provided by the manufacturer. Briefly, ELT3 cells were treated with MG132 at various concentrations (0, 0.5, 1 and 2 μM) for 24 or 48 h at 37˚C in 6-well plates at a density of $5x10^4$ cells per well. Following treatment, the cells were trypsinized to detach them from the wells and harvested by centrifugation at 300 x g for 5 min at room temperature. The cell pellets were then resuspended in fresh media to prepare them for staining. Subsequently, 100 μl of Muse® Annexin V & Dead Cell reagent was added to the cell suspension. The cells were then incubated for 20 min at room temperature in the dark to allow proper staining of the apoptotic and dead cells. Following incubation, the stained cells were analyzed using a Guava® Muse® Cell Analyzer (cat. no. 0500-3115; Cytek Biosciences).

Flow cytometric evaluation of cell cycle distribution. A Muse® Cell Cycle Kit (cat. no. MCH100106; Cytek Biosciences) was used to analyze the cell cycle phases of the samples. Initially, cells were harvested and centrifuged at 300 x g for 5 min at room temperature to form a pellet, which was then fixed in 70% ethanol at -20˚C for 3 h. Following fixation, the cells were stained at room temperature using the Muse® Cell Cycle Reagent and incubated in darkness for 30 min to ensure proper staining. The stained samples were analyzed using a Guava®

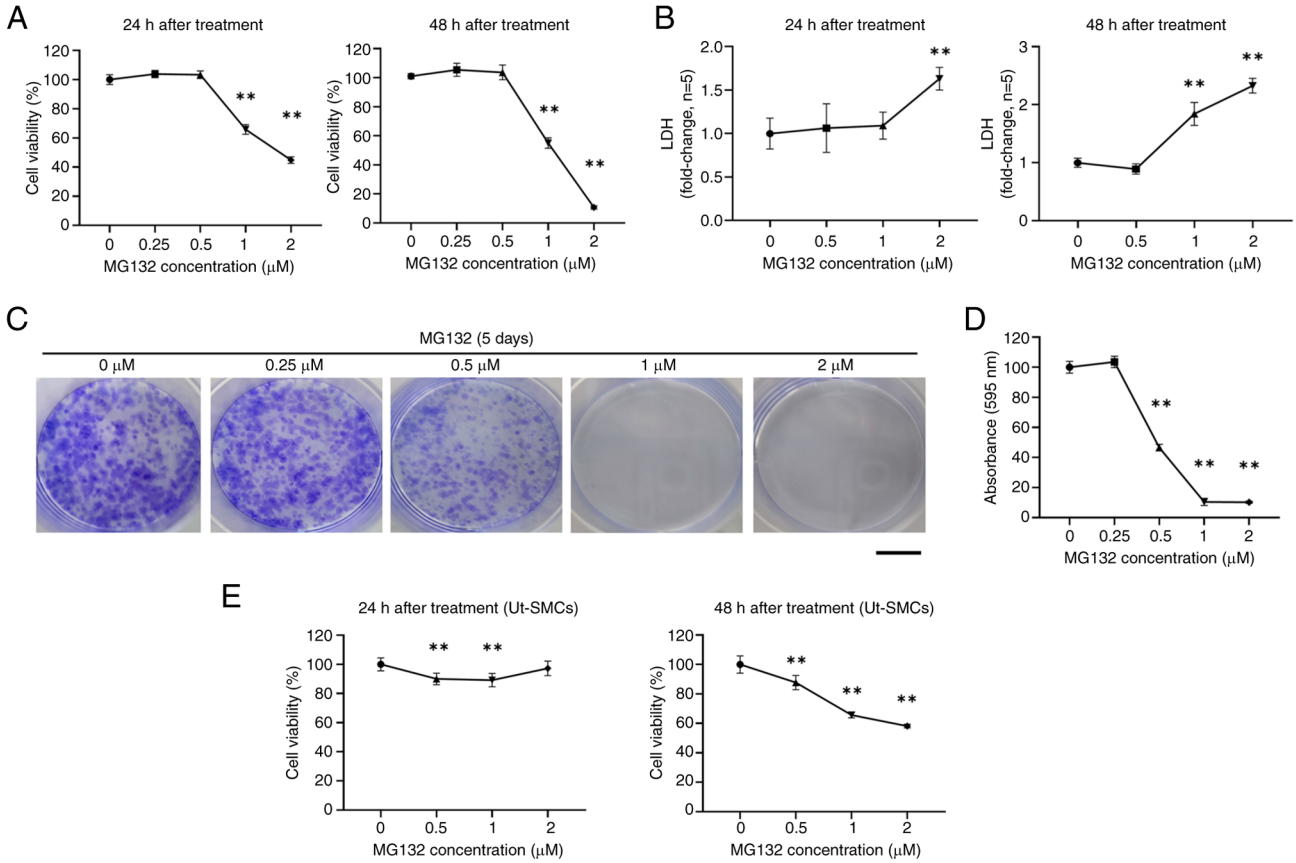

Figure 1. MG132 reduces the cell viability, increases the release of LDH, and impairs colony formation in ELT3 cells. (A and B) ELT3 cells were treated with MG132 at the indicated concentrations for 24 and 48 h, followed by MTT cell viability and LDH release assays. (C) Representative images of the colonies stained using crystal violet (black scale bar, 10 mm). (D) The absorbance of the crystal violet-stained cells was measured at 595 nm after lysis. (E) Ut-SMCs were treated with various concentration (0-2 μM) of MG132 for 24 or 48 h, and cell viability was measured using the MTT assay. Data are presented as the mean ± standard deviation. All experiments were conducted in triplicate. **P<0.01 compared with the control group. MG132, carbobenzoxyl-L-leucyl-L-l eucyl-L-leucine; LDH, Lactate dehydrogenase; Ut-SMCs, uterine smooth muscle cells. MG132, carbobenzoxyl-L-leucyl-L-leucyl-L-leucine; LDH, lactate dehydrogenase; ELT3, Eker leiomyoma tumor-3; Ut-SMCs, uterine smooth muscle cells.

Muse® Cell Analyzer to determine the distribution of cells across the different phases of the cell cycle.

ROS quantification using flow cytometry. ROS production was quantified via flow cytometry using a Muse® Oxidative Stress Kit (cat. no. MCH100111; Cytek Biosciences), following the manufacturer's guidelines. In summary, ELT3 cells were seeded in 6-well plates at a density of $5x10^4$ cells per well and cultured at 37˚C for 24 h. The cells were treated with 0, 1, or 2 μM MG132 in fresh media at 37˚C for 24 and 48 h. Following treatment, the cells were detached and resuspended in 1X Assay Buffer, followed by the addition of the Muse® Oxidative Stress Reagent working solution. The samples were incubated at 37˚C for 30 min before being analyzed with a Guava® Muse® Cell Analyzer.

Protein preparation and western blot analysis. Protein extraction and western blotting were conducted following a previously published protocol (27). For detection, the following primary antibodies were used: LC3B (cat. no. 2775S), p27 (cat. no. 3686T), phosphorylated (p)-p44/42 MAPK (Erk1/2) (cat. no. 9106S), p44/42 MAPK (cat. no. 4695S), poly(ADP-ribose) polymerase 1 (PARP) (cat. no. 9542S), caspase-3 (cat. no. 9665S), and cleaved caspase-3 (cat. no. 9664S) all from Cell Signaling Technology, as well as p21 (cat. no. sc-6246) and heat shock protein 90 (cat. no. sc-13119) from Santa Cruz Biotechnology, Inc. Heat shock protein 90 was used as a loading control to verify equal protein loading across the lanes. The protein signals were visualized using the Immobilon ECL Ultra Western HRP Substrate (cat. no. WBKLS0100; MilliporeSigma) and analyzed with an Azure c280 chemi-luminescent imaging system (Azure Biosystems Ins.). Densitometric analysis of the resulting images was then performed using ImageJ 1.53a software (National Institutes of Health).

Statistical analyses. Statistical analyses were conducted using GraphPad Prism software (version 8.0; Dotmatics). Data are presented as the mean ± standard deviation. A one-way analysis of variance (ANOVA) was used to compare multiple groups, followed by Tukey's post hoc test or Dunnett's multiple comparison test as appropriate. P<0.05 was considered to indicate a statistically significant difference.

Results

MG132 inhibits ELT3 cell viability and colony formation. The cytotoxic effects of MG132 on ELT3 uterine leiomyoma cells

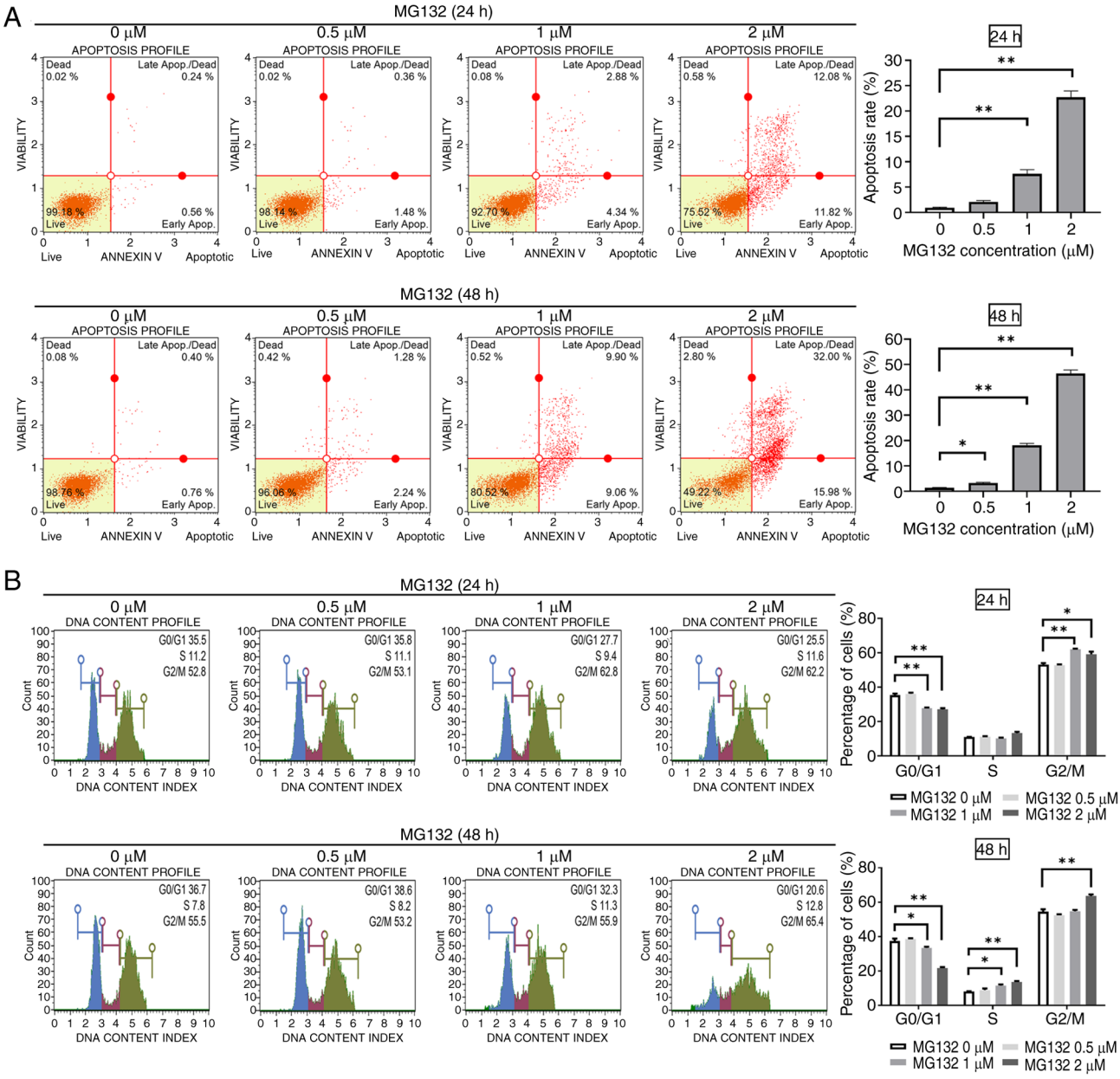

Figure 2. Effects of MG132 on cell apoptosis and cell cycle distribution in ELT3 Cells. (A) Apoptosis rates were measured via Annexin V staining after 24 and 48 h of treatment with MG132 at the indicated concentrations. (B) DNA content was measured to determine the percentage of cells in the G_0/G_1, S, and G_2/M phases after the treatment with MG132 for 24 and 48 h at the indicated concentrations. Three independent experiments were performed and exhibited similar results. Data are presented as the mean ± standard deviation. *P<0.05 and **P<0.01 compared with the control group. MG132, carbobenzoxyl-L-leucyl-L-leucyl-L-leucine; ELT3, Eker leiomyoma tumor-3.

were investigated first by assessing cell viability using MTT assays and LDH activity through LDH release assays. The results revealed that MG132 significantly reduced cell viability and increased LDH activity at 24 and 48 h. Specifically, cell viability was decreased to ~44.8% using 2 μM MG132 after 24 h. It was further decreased to ~10.7% after 48 h (Fig. 1A). LDH activity was significantly increased, with a 1.63-fold change using 2 μM MG132 after 24 h and a 2.32-fold change after 48 h (Fig. 1B). To further evaluate the effects of MG132, a colony formation assay was performed. Crystal violet staining revealed that colonies treated with MG132 at 0.25, 0.5, 1 and 2 μM for 5 days were decreased compared with the control group (Fig. 1C). Additionally, the MG132 treatment of 1 and 2 μM reduced the absorbance at 595 nm by ~90% (Fig. 1D). By contrast, compared with ELT3 cells, treatment of normal Ut-SMCs with MG132 for 24 and 48 h resulted in a lesser reduction in viability (Fig. 1E). These findings indicated that high concentrations of MG132 decrease cell viability, increase LDH release, and significantly impair colony formation in ELT3 cells.

MG132 induces apoptosis and G_2/M phase arrest in ELT3 cells. To examine whether ELT3 cells undergo apoptosis, cells were treated with MG132 at concentrations of 0.5, 1 or 2 μM for 24 and 48 h. Apoptosis was measured using Annexin V staining and analyzed by flow cytometry. Significant increases in apoptosis were observed at 1 and 2 μM after 24 h of treatment (Fig. 2A, upper images). Similar patterns were observed

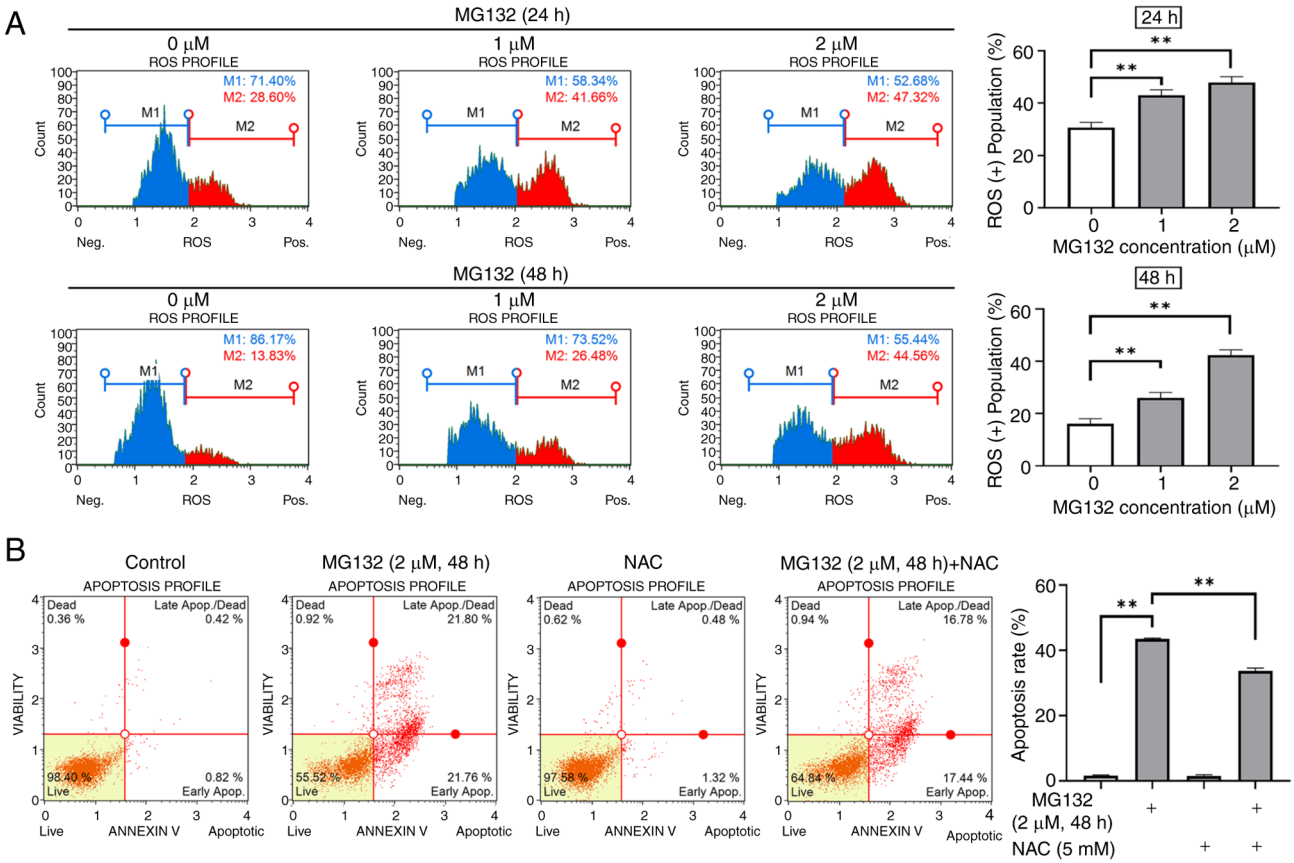

Figure 3. MG132 induces ROS production and apoptosis in ELT3 cells. (A) ROS production was measured using a Muse® Oxidative Stress kit, and the typical ROS profile plots (left images) and the statistical analysis (right images) are demonstrated for each treatment condition. (B) Apoptosis was measured in ELT3 cells treated with MG132 (2 μM) in the presence or absence of NAC (5 mM) for 48 h. The data are expressed as the mean ± standard deviation; n=3. **P<0.01. MG132, carbobenzoxyl-L-leucyl-L-leucyl-L-leucine; ROS, reactive oxygen species; ELT3, Eker leiomyoma tumor-3; NAC, N-acetylcysteine; ROS, reactive oxygen species.

after 48 h of treatment (Fig. 2A, lower images). To investigate whether MG132-mediated inhibition of cell proliferation was related to cell cycle arrest, ELT3 cells were treated with varying concentrations of MG132 for 24 and 48 h. Cell cycle profiles were assessed using a Guava® Muse® Cell Analyzer. MG132 significantly increased the cell population in the G_2/M phase while reducing the cell population in the G_0/G_1 phase after 24 and 48 h of treatment (Fig. 2B). These results confirmed that MG132 induces apoptosis in ELT3 cells in a concentration- and time-dependent manner and causes cell cycle arrest at the G_2/M phase.

MG132 increases ROS production in ELT3 cells. Excessive accumulation of ROS in cells can lead to oxidative stress, damaging nucleic acids, lipids, proteins, membranes, and mitochondria (28). To assess whether MG132 increases ROS levels in ELT3 cells, the cells were treated with different concentrations of MG132 (0, 1 and 2 μM) for 24 and 48 h, and then analyzed using a Guava® Muse® Cell Analyzer. ROS levels were 30.68, 42.97 and 47.88% in the control and the MG132-treated ELT3 cells at MG132 concentrations of 0, 1 and 2 μM for 24 h, respectively (Fig. 3A, upper images), and after 48 h of MG132 treatment, the ROS levels were 16.07, 25.95 and 42.38%, respectively (Fig. 3A, bottom images). To further determine whether ROS production was involved in MG132-induced apoptosis, ELT3 cells were treated with 2 μM MG132 for 48 h in the presence or absence of 5 mM NAC. NAC is a known antioxidant (29). NAC effectively reduced MG132-induced apoptosis in ELT3 cells (Fig. 3B). These results indicated that MG132 induces ROS generation, which leads to ROS-mediated apoptosis in ELT3 cells.

Effect of MG132 on the expression of proteins related to cell proliferation and apoptosis in ELT3 cells. To study the mechanism of MG132, western blotting was used to detect the cell cycle-regulatory proteins p21 and p27, as well as the phosphorylation of ERK, which is essential for its activation. MG132 significantly increased the p21 protein expression at 1 and 2 μM at 24 h, but decreased the expression at 2 μM at 48 h (Fig. 4A; lanes 2 and 3 at 24 h and lanes 5 and 6 at 48 h). In addition, untreated ELT3 cells had elevated levels of p27 and ERK phosphorylation at 48 h, whereas MG132 treatment decreased p27 expression and ERK phosphorylation in a dose-dependent manner at 48 h (Fig. 4A; lanes 4 to 6). To understand how MG132 triggers apoptosis in ELT3 cells, caspase-3, cleaved caspase-3, and PARP expression levels were analyzed. MG132 increased the cleaved caspase-3 to total caspase-3 ratio and the cleaved PARP to total PARP ratio at 2 μM for 24 and 48 h compared to the control (Fig. 4B). These findings indicated that MG132 modulates cell cycle- and apoptosis-related proteins, leading to reduced proliferation and increased apoptosis in ELT3 cells.

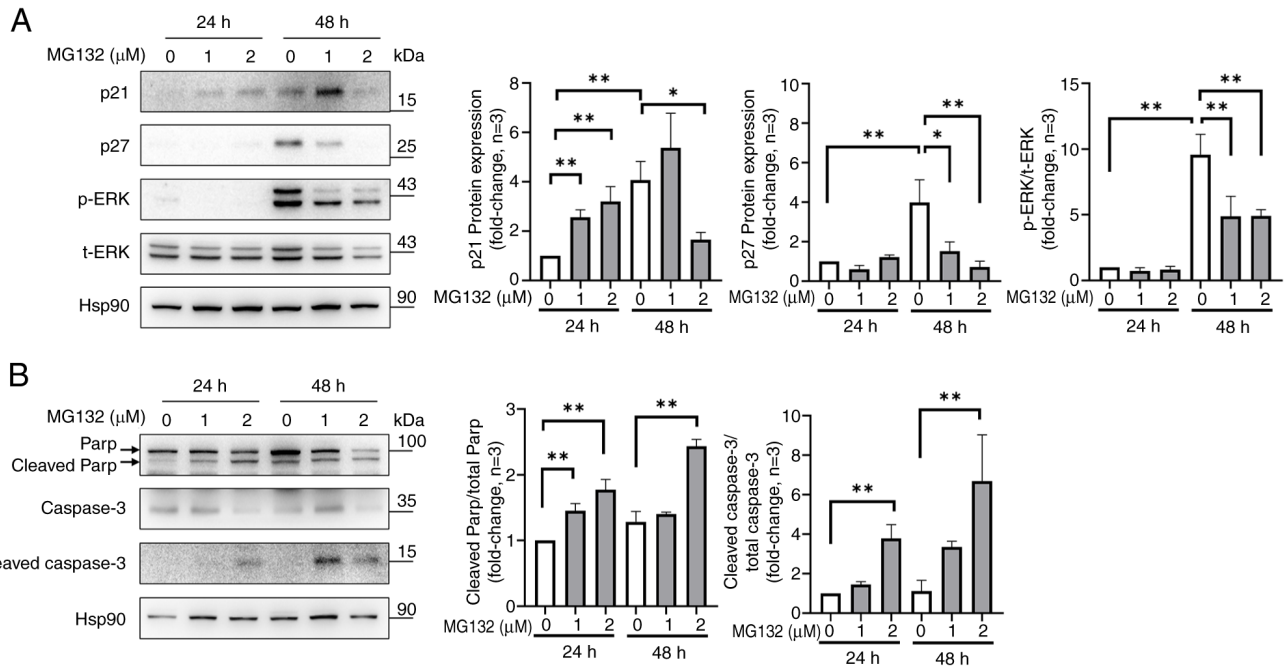

Figure 4. Effects of MG132 on cell proliferation- and apoptosis-related proteins in ELT3 cells. (A) Western blot analysis of p21, p27, p-ERK, and ERK, with bar graphs revealing the p21 and p27 ratios relative to Hsp90. (B) The effect of MG132 on caspase-3 activation and PARP cleavage was also assessed. Data are presented as the mean ± standard deviation from three independent experiments. *P<0.05 and **P<0.01 compared with each group as indicated in the graphs. MG132, carbobenzoxyl-L-leucyl-L-leucyl-L-leucine; ELT3, Eker leiomyoma tumor-3; ERK, extracellular signal-regulated kinase; Hsp90, heat shock protein 90; PARP, poly(ADP-ribose) polymerase 1; p, phosphorylated; t, total.

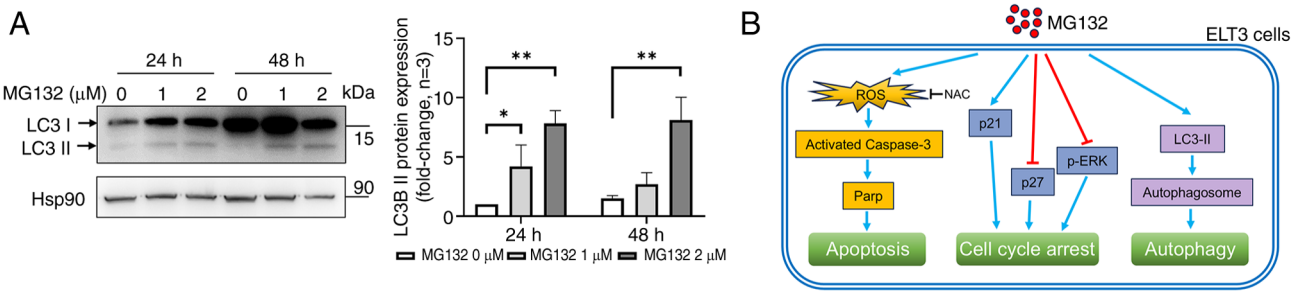

Figure 5. MG132 affects LC3 expression in ELT3 cells. (A) LC3 I/II levels in ELT3 cells treated with or without MG132 for 24 and 48 h were analyzed by western blot analysis. Band intensities were quantified using ImageJ. (B) A schematic representation illustrating the various cellular pathways through which MG132 exerts its antitumor effects in ELT3 cells. Data are presented as the mean ± standard deviation from three independent experiments. *P<0.05 and **P<0.01 compared with each group as indicated in the graphs. MG132, carbobenzoxyl-L-leucyl-L-leucyl-L-leucine; LC3, microtubule-associated protein 1 light chain 3; ELT3, Eker leiomyoma tumor-3; Hsp90, heat shock protein 90; ROS, reactive oxygen species; PARP, poly(ADP-ribose) polymerase 1.

MG132 induces autophagy in ELT3 cells by activating LC3. Autophagy is a crucial process that maintains cellular homeostasis under normal and stress conditions (30). To evaluate autophagy induction, western blotting was used to measure LC3 protein expression, a key protein involved in autophagosome formation (30). The conversion of LC3 I to LC3 II, a marker of autophagy, was observed after treating ELT3 cells with 1 and 2 μM MG132 for 24 and 48 h, as shown by the increased LC3 II levels (Fig. 5A). These findings indicated that MG132 triggers autophagy or a form of programmed cell death in ELT3 cells.

Discussion

The findings of the present study are summarized and illustrated in Fig. 5B. The present study offered important insights into the potential use of MG132 to treat ELT3 uterine leiomyoma cells, which serve as a model for a common and often troubling gynecological condition. These results demonstrated that MG132 significantly reduced cell growth and colony formation, caused cell death, stopped cells from progressing through the G_2/M phase of the cell cycle, and increased ROS production. These results suggest that MG132 and similar proteasome inhibitors could effectively target leiomyoma cells. Furthermore, the present research improved the understanding of how MG132 impacts important proteins involved in the cell cycle and cell death, including p21, p27, ERK, and caspase-3. Additionally, the present study demonstrated that MG132 induces autophagy, as indicated by the increased conversion of LC3 I to LC3 II (Fig. 5). This is crucial as it highlights the potential of MG132 for regulating the survival of uterine leiomyomas by demonstrating the possibility of targeting the proteasome.

In several studies, MG132 has been revealed to play a crucial role in inducing apoptosis. MG132 disrupts protein degradation within cells by affecting the ubiquitin-proteasome pathway, leading to increased cellular stress and modulating inflammatory responses (31,32). Specifically, MG132 can induce apoptosis through the mitochondrial pathway and activate cell death pathways by causing an accumulation of ROS within the cells (25). Additionally, MG132 has been demonstrated to suppress the expression of anti-apoptotic proteins, such as Bcl-2, and to promote apoptosis by activating apoptosis-related proteins, such as caspase-3 (33). Moreover, numerous studies have revealed that MG132 can cause cells to arrest in the G_2/M phase of the cell cycle (34,35). During this phase, cells undergo DNA damage checks and repair processes, and MG132 interferes with the degradation of proteins essential for this process, leading to cell cycle arrest. For example, cyclin-dependent kinase inhibitors (CDK inhibitors), such as p21, are stabilized by MG132, causing cells to halt at the G_2/M phase (35).

The western blot analysis revealed that MG132 increased p21 expression at 24 h but decreased the expression at 48 h, indicating a complex regulatory effect on cell cycle progression. In addition, MG132 treatment decreased p27 expression and ERK phosphorylation, both of which are associated with cell proliferation. These findings suggest that the anti-proliferative effects of MG132 are more likely related to changes in p21 and ERK phosphorylation rather than changes in p27. Additionally, the activation of caspase-3 and the cleavage of PARP further confirmed the pro-apoptotic effects of MG132 in ELT3 cells. This similarity between the results of the present study and previous studies suggests that MG132 and other proteasome inhibitors could be effective in targeting leiomyoma cells, highlighting their potential as promising treatments in cancer therapy (33,35).

Notably, MG132 was revealed to induce autophagy in ELT3 cells, as evidenced by the increased conversion of LC3 I to LC3 II. Autophagy is a cellular process that can either promote survival or lead to cell death, depending on the context (36,37). In MCF-7 breast cancer cells, MG132-induced autophagy was linked to endoplasmic reticulum stress (38). Similarly, in A549 human lung adenocarcinoma cells, MG132 treatment enhanced autophagy, marked by the upregulation of LC3B and the conversion of LC3B-I to lipidated LC3B-II, aiding the degradation of the polyubiquitinated AGR2 protein (39). In N2a cells and primary neurons, MG132 also triggered a time-dependent increase in LC3-II levels (40). While autophagy initially acts as a protective mechanism against MG132-induced proteotoxic stress, its persistence may lead to autophagic cell death, as suggested by the significant rise in LC3 II levels observed in the present study. This dual role of autophagy highlights the complex balance between survival and death mechanisms in response to MG132.

Despite the promising results, the present study has several limitations. First, while MG132 significantly affected ELT3 cells *in vitro*, its efficacy and safety *in vivo* remain untested. Using a single cell line limits the generalizability of these findings, given the heterogeneity of uterine leiomyomas. Although MG132 increased ROS production and induced apoptosis, the present study did not fully elucidate the specific pathways linking ROS to cell death. Additionally, the present study did not entirely rule out the involvement of other forms of programmed cell death. Prolonged treatment with MG132 can also decrease the viability of normal Ut-SMCs, indicating potential non-specific effects on normal tissues. Thus, further studies are required to determine the optimal concentration and exposure time of MG132, as well as strategies to minimize off-target effects and ensure selective toxicity toward leiomyoma cells. These additional experiments, including *in vivo* studies, are essential to assess the therapeutic potential and safety of MG132 as a treatment for uterine leiomyomas.

In conclusion, the findings of the present study suggest that MG132 exerts its anti-proliferative effects on ELT3 cells through multiple mechanisms, including the induction of apoptosis, cell cycle arrest, ROS production, and autophagy. The results highlight the potential of MG132 in controlling the survival of uterine leiomyomas by demonstrating the ability to target the proteasome. However, further *in vivo* studies are necessary to fully evaluate the therapeutic efficacy and safety of MG132 in treating uterine leiomyomas.

Acknowledgements

Not applicable.

Funding

The present study was supported by a research fund from Chosun university (grant no. K208554002).

Availability of data and materials

The data generated in the present study may be requested from the corresponding author.

Authors' contributions

HJ and SRY designed the experiments and revised the manuscript. HL and SBL conducted the experiments and wrote the manuscript. HJ and SRY performed the experiments and data analyses. All authors read and approved the final manuscript. HL and HJ confirm the authenticity of all the raw data.

Ethics approval and consent to participate

Not applicable.

Patient consent for publication

Not applicable.

Competing interests

The authors declare that they have no competing interests.

References

1. Stewart EA, Laughlin-Tommaso SK, Catherino WH, Lalitkumar S, Gupta D and Vollenhoven B: Uterine fibroids. Nat Rev Dis Primers 2: 16043, 2016.

2. Sohn GS, Cho S, Kim YM, Cho CH, Kim MR and Lee SR; Working Group of Society of Uterine Leiomyoma: Current medical treatment of uterine fibroids. Obstet Gynecol Sci 61: 192-201, 2018.
3. Cermik D, Arici A and Taylor HS: Coordinated regulation of HOX gene expression in myometrium and uterine leiomyoma. Fertil Steril 78: 979-984, 2002.
4. Okoro CC, Ikpeze OC, Eleje GU, Udigwe GO, Ezeama CO, Ugboaja JO, Enechukwu CI, Umeononihu OS, Ogabido CA, Oguejiofor CB, *et al*: Association between serum vitamin D status and uterine leiomyomas: A case-control study. Obstet Gynecol Sci 67: 101-111, 2024.
5. De La Cruz MS and Buchanan EM: Uterine fibroids: Diagnosis and treatment. Am Fam Physician 95: 100-107, 2017.
6. Lee MJ, Yun BS, Seong SJ, Kim ML, Jung YW, Kim MK, Bae HS, Kim DH and Hwang JY: Uterine fibroid shrinkage after short-term use of selective progesterone receptor modulator or gonadotropin-releasing hormone agonist. Obstet Gynecol Sci 60: 69-73, 2017.
7. Navarro A, Bariani MV, Yang Q and Al-Hendy A: Understanding the impact of uterine fibroids on human endometrium function. Front Cell Dev Biol 9: 633180, 2021.
8. Angioni S, D'Alterio MN and Daniilidis A: Highlights on medical treatment of uterine fibroids. Curr Pharm Des 27: 3821-3832, 2021.
9. Lee S and Stewart EA: New treatment options for nonsurgical management of uterine fibroids. Curr Opin Obstet Gynecol 35: 288-293, 2023.
10. Duhan N: Current and emerging treatments for uterine myoma-an update. Int J Womens Health 3: 231-241, 2011.
11. Choe YS, Lee WM, Choi JS, Bae J, Eom JM and Choi E: Clinical characteristics of patients with leiomyoma who undergo surgery after high intensity focused ultrasound (HIFU). Obstet Gynecol Sci 62: 258-263, 2019.
12. Yerezhepbayeva M, Terzic M, Aimagambetova G and Crape B: Comparison of two invasive non-surgical treatment options for uterine myomas: Uterine artery embolization and magnetic resonance guided high intensity focused ultrasound-systematic review. BMC Womens Health 22: 55, 2022.
13. Yang CH, Gonzalez-Angulo AM, Reuben JM, Booser DJ, Pusztai L, Krishnamurthy S, Esseltine D, Stec J, Broglio KR, Islam R, *et al*: Bortezomib (VELCADE) in metastatic breast cancer: Pharmacodynamics, biological effects, and prediction of clinical benefits. Ann Oncol 17: 813-817, 2006.
14. Engel RH, Brown JA, Von Roenn JH, O'Regan RM, Bergan R, Badve S, Rademaker A and Gradishar WJ: A phase II study of single agent bortezomib in patients with metastatic breast cancer: A single institution experience. Cancer Invest 25: 733-737, 2007.
15. Cresta S, Sessa C, Catapano CV, Gallerani E, Passalacqua D, Rinaldi A, Bertoni F, Viganò L, Maur M, Capri G, *et al*: Phase I study of bortezomib with weekly paclitaxel in patients with advanced solid tumours. Eur J Cancer 44: 1829-1834, 2008.
16. Ramirez PT, Landen CN Jr, Coleman RL, Milam MR, Levenback C, Johnston TA and Gershenson DM: Phase I trial of the proteasome inhibitor bortezomib in combination with carboplatin in patients with platinum- and taxane-resistant ovarian cancer. Gynecol Oncol 108: 68-71, 2008.
17. Yang H, Zonder JA and Dou QP: Clinical development of novel proteasome inhibitors for cancer treatment. Expert Opin Investig Drugs 18: 957-971, 2009.
18. Lee DH and Goldberg AL: Proteasome inhibitors: Valuable new tools for cell biologists. Trends Cell Biol 8: 397-403, 1998.
19. Han YH, Moon HJ, You BR and Park WH: The effect of MG132, a proteasome inhibitor on HeLa cells in relation to cell growth, reactive oxygen species and GSH. Oncol Rep 22: 215-221, 2009.
20. Guo N and Peng Z: MG132, a proteasome inhibitor, induces apoptosis in tumor cells. Asia Pac J Clin Oncol 9: 6-11, 2013.
21. Tarjányi O, Haerer J, Vecsernyés M, Berta G, Stayer-Harci A, Balogh B, Farkas K, Boldizsár F, Szeberényi J and Sétáló G Jr: Prolonged treatment with the proteasome inhibitor MG-132 induces apoptosis in PC12 rat pheochromocytoma cells. Sci Rep 12: 5808, 2022.
22. Yang W, Monroe J, Zhang Y, George D, Bremer E and Li H: Proteasome inhibition induces both pro- and anti-cell death pathways in prostate cancer cells. Cancer Lett 243: 217-227, 2006.
23. Yan H, Ma YL, Gui YZ, Wang SM, Wang XB, Gao F and Wang YP: MG132, a proteasome inhibitor, enhances LDL uptake in HepG2 cells in vitro by regulating LDLR and PCSK9 expression. Acta Pharmacol Sin 35: 994-1004, 2014.
24. Zhang Y, Yang B, Zhao J, Li X, Zhang L and Zhai Z: Proteasome inhibitor carbobenzoxy-L-Leucyl-L-leucyl-L-leucinal (MG132) enhances therapeutic effect of paclitaxel on breast cancer by inhibiting nuclear factor (NF)-κB signaling. Med Sci Monit 24: 294-304, 2018.
25. Han YH and Park WH: MG132 as a proteasome inhibitor induces cell growth inhibition and cell death in A549 lung cancer cells via influencing reactive oxygen species and GSH level. Hum Exp Toxicol 29: 607-614, 2010.
26. Duan W, Guo Y, Jiang H, Yu X and Li C: MG132 enhances neurite outgrowth in neurons overexpressing mutant TAR DNA-binding protein-43 via increase of HO-1. Brain Res 1397: 1-9, 2011.
27. Joung H and Liu H: 2-D08 mediates notable anticancer effects through multiple cellular pathways in uterine leiomyosarcoma cells. Oncol Rep 52: 97, 2024.
28. Cenini G, Lloret A and Cascella R: Oxidative stress and mitochondrial damage in neurodegenerative diseases: From molecular mechanisms to targeted therapies. Oxid Med Cell Longev 2020: 1270256, 2020.
29. Zhitkovich A: N-acetylcysteine: Antioxidant, aldehyde scavenger, and more. Chem Res Toxicol 32: 1318-1319, 2019.
30. Aman Y, Schmauck-Medina T, Hansen M, Morimoto RI, Simon AK, Bjedov I, Palikaras K, Simonsen A, Johansen T, Tavernarakis N, *et al*: Autophagy in healthy aging and disease. Nat Aging 1: 634-650, 2021.
31. Ortiz-Lazareno PC, Hernandez-Flores G, Dominguez-Rodriguez JR, Lerma-Diaz JM, Jave-Suarez LF, Aguilar-Lemarroy A, Gomez-Contreras PC, Scott-Algara D and Bravo-Cuellar A: MG132 proteasome inhibitor modulates proinflammatory cytokines production and expression of their receptors in U937 cells: Involvement of nuclear factor-kappaB and activator protein-1. Immunology 124: 534-541, 2008.
32. Park HS, Jun do Y, Han CR, Woo HJ and Kim YH: Proteasome inhibitor MG132-induced apoptosis via ER stress-mediated apoptotic pathway and its potentiation by protein tyrosine kinase p56lck in human Jurkat T cells. Biochem Pharmacol 82: 1110-1125, 2011.
33. Westerberg CM, Hägglund H and Nilsson G: Proteasome inhibition upregulates Bim and induces caspase-3-dependent apoptosis in human mast cells expressing the Kit D816V mutation. Cell Death Dis 3: e417, 2012.
34. Kim OH, Lim JH, Woo KJ, Kim YH, Jin IN, Han ST, Park JW and Kwon TK: Influence of p53 and p21Waf1 expression on G2/M phase arrest of colorectal carcinoma HCT116 cells to proteasome inhibitors. Int J Oncol 24: 935-941, 2004.
35. Zanotto-Filho A, Braganhol E, Battastini AM and Moreira JC: Proteasome inhibitor MG132 induces selective apoptosis in glioblastoma cells through inhibition of PI3K/Akt and NFkappaB pathways, mitochondrial dysfunction, and activation of p38-JNK1/2 signaling. Invest New Drugs 30: 2252-2262, 2012.
36. Jung S, Jeong H and Yu SW: Autophagy as a decisive process for cell death. Exp Mol Med 52: 921-930, 2020.
37. Liu S, Yao S, Yang H, Liu S and Wang Y: Autophagy: Regulator of cell death. Cell Death Dis 14: 648, 2023.
38. Bao W, Gu Y, Ta L, Wang K and Xu Z: Induction of autophagy by the MG-132 proteasome inhibitor is associated with endoplasmic reticulum stress in MCF-7 cells. Mol Med Rep 13: 796-804, 2016.
39. Wang D, Xu Q, Yuan Q, Jia M, Niu H, Liu X, Zhang J, Young CY and Yuan H: Proteasome inhibition boosts autophagic degradation of ubiquitinated-AGR2 and enhances the antitumor efficiency of bevacizumab. Oncogene 38: 3458-3474, 2019.
40. Guo F, He XB, Li S and Le W: A central role for phosphorylated p38α in linking proteasome inhibition-induced apoptosis and autophagy. Mol Neurobiol 54: 7597-7609, 2017.